International Food Research Journal 32(1): 108 - 120 (February 2025)
Journal homepage: *http://www.ifrj.upm.edu.my*

Effect of blanching conditions on physico-chemical characteristics of cocoa pod husk

[1,2]Anoraga, S. B., [1,3]*Shamsudin, R., [4]Hamzah, M. H., [5]Sharif, S. and [6]Saputro, A. D.

[1]Department of Process and Food Engineering, Faculty of Engineering, Universiti Putra Malaysia, Selangor, Malaysia
[2]Department of Bioresources Technology and Veterinary, Universitas Gadjah Mada Vocational College, Yogyakarta, Indonesia
[3]Laboratory of Halal Services, Halal Products Research Institute, Universiti Putra Malaysia, Selangor, Malaysia
[4]Department of Biological and Agricultural Engineering, Faculty of Engineering, Universiti Putra Malaysia, Selangor, Malaysia
[5]Malaysian Cocoa Board, Kota Kinabalu, Sabah
[6]Department of Agricultural Engineering, Faculty of Agricultural Technology, Universitas Gadjah Mada, Yogyakarta, Indonesia

Article history

Received:
21 May 2024
Received in revised form:
23 November 2024
Accepted:
29 November 2024

Keywords

optimisation, pre-treatment, physicochemical, proximate, cocoa pod husk

Abstract

Effective post-harvest handling and grading of cocoa fruit require a comprehensive understanding of its physical and chemical characteristics. The cocoa pod husk (CPH), a significant by-product, has potential applications due to its valuable chemical properties. The present work thus aimed to (1) characterise the physico-chemical properties of cocoa fruit and its husk, (2) develop predictive models for cocoa fruit mass based on physical parameters, and (3) optimise short-time blanching conditions to enhance the chemical quality of CPH. The methodology included measuring physical parameters (weight, dimensions, roundness, volume, surface area, and projected area), and developing predictive models for cocoa fruit mass using linear, quadratic, S-curve, and power models. Chemical analyses of CPH involved determining pH, biomass composition, total phenolic content, antioxidant activity, and dietary fibre content. Optimisation of blanching conditions was conducted using a response surface methodology with temperature and time as variables. Results indicated that a non-linear model based on projected area effectively predicted cocoa fruit mass, with the prolate spheroid volume model offering the highest accuracy. Optimal blanching conditions (79°C for 12.5 sec) yielded 36.19% crude fibre and 4.189% protein, with crude fibre content influenced by temperature, and a significant temperature-time interaction effect on protein content ($p < 0.05$). These findings suggested that CPH can be repurposed as a functional food ingredient rich in phenolics, antioxidants, and dietary fibre, offering practical applications for value-added agricultural waste recovery.

List of abbreviations

ANOVA: Analysis of Variance; CCD: Central Composite Design; CPA: criterion-projected areas; CPH: cocoa pod husk; Dg: geometric mean diameter; DPPH: 1,1-diphenyl-2-picrylhydrazyl; GAE: gallic acid equivalents; L: length; M: mass; PAL: projected areas to length; PAT: projected areas to thickness; PAW: projected areas to width; R^2: regression coefficient; RSM: Response Surface Methodology; SAsp: surface area; SD: standard deviation; SEE: standard error of estimate; T: thickness; Vobl: volumes oblate shape; Vpro: volumes prolate spheroid; W: width; and Φ: sphericity.

DOI
https://doi.org/10.47836/ifrj.32.1.08

Introduction

Cocoa (*Theobroma cacao* L.) is manually processed by small farms. The extraction of beans and pulps from cocoa pods is a delicate processing requiring considerable skill (Andrade Sodré *et al*., 2019). Understanding the physical characteristics of cocoa pods is crucial to the design of post-harvest systems for handling, sorting, and processing cocoa pods. Dimension, mass, volume, and projected area

*Corresponding author.
Email: rosnahs@upm.edu.my

are among the parameters vital to the design of processing systems (Azman *et al*., 2020), and a technology designed based on mass categorisation could be more cost-effective than designs based on other parameters, especially for cocoa pods of varying sizes. Such technology can reduce grading time and labour cost. Therefore, developing a model for predicting cocoa pod weight by using variables, such as length, thickness, width, and projected area, are needed (Khoshnam *et al*., 2007).

Cocoa pod husk (CPH) is a by-product of the cocoa fruit and chocolate production industries. This surplus waste is typically utilised as animal feed, but frequently remains unused, and commonly discarded in the soil, resulting in substantial environmental issues, potentially contaminating the plantations, and increasing the risk of infectious diseases (Hamzah *et al*., 2024). Various pre-treatment methods are employed to enhance the utilisation and value of CPH as biomass waste, and improve its quality. Drying and fermentation (Dahunsi *et al*., 2019), palletisation (Syamsiro *et al*., 2012), extraction (Belwal *et al*., 2022), and size reduction (Wibisono *et al*., 2021) contribute to improving the quality and potential applications of CPH.

Blanching is a common treatment applied to fruit husk and peel. Before drying, enzymes, such as peroxidase and polyphenol oxidase are rendered inactive by blanching in hot water (Magangana *et al*., 2021). The effect of blanching on the proximate composition of fruit husk and peel can considerably affect the nutritional value, colour, texture, and destruction of enzymes (Bhardwaj *et al*., 2022). The effect of blanching on the proximate composition of fruit husk and peel can vary by type of fruit and blanching duration.

However, the information on the effects of short blanching time and temperature on the proximate composition of CPH remains limited. The proximate composition is a critical attribute of CPH, as blanching can significantly impact its nutritional value, colour, texture, and enzyme activity (Kim *et al*., 2020). Although few studies have investigated the impact of blanching parameters on CPH composition, these effects are essential for optimising CPH as a valuable raw material in nutrient-rich food ingredients. Temperature and blanching time are essential factors in optimising the blanching process for CPH due to their impact on enzyme inactivation, nutrient preservation, and overall quality. Higher temperatures accelerate enzyme inactivation, crucial for preventing degradation, yet excessively high temperatures risk nutrient loss and textural changes (Xu, 2017). Similarly, blanching time affects both enzyme inactivation and nutrient retention—insufficient time can result in incomplete inactivation, while prolonged exposure can cause nutrient leaching (Nhi *et al*., 2022). To achieve this, we applied a central composite design (CCD) within the framework of response surface methodology (RSM), which allows efficient exploration of temperature and blanching time interactions across a multidimensional response plane. This approach was chosen for its robustness in optimising processing conditions with minimal experimental runs, ensuring precise modelling of factor interactions on proximate composition. The objective of the present work was to enhance the protein, crude fibre, ash, and moisture contents of CPH through optimised short-time hot-water blanching. Key physicochemical properties, including proximate composition, antioxidant activity (1,1-diphenyl-2-picrylhydrazyl, DPPH), total phenolic content (TPC), and dietary fibre content, were analysed. Additionally, the best predictive model for cocoa fruit mass based on physical parameters was identified. The present work aimed to provide valuable insights for improving CPH handling, waste minimisation, by-product utilisation, and food security efforts.

Materials and methods

Sample preparation

Cocoa fruits were harvested at the same maturity level from the Malaysian Cocoa Board farm in Bagan Datuk, Perak, Malaysia, using three clones: KKM 22, MCBC 1, and PBC 123. Only fresh, healthy, and uninjured pods were selected, while damaged samples were excluded during standardisation (Rossetti *et al*., 2022). Analytical-grade reagents used were sodium hydroxide (Merck, Germany), ethanol (≥ 99.8%, Sigma-Aldrich, USA), and *n*-hexane (Fisher Scientific, USA). For dietary fibre analysis, enzymes such as α-amylase, protease, and amyloglucosidase (Megazyme, Ireland) were used. All experiments were conducted in the laboratory at room temperature.

Physical properties

Cocoa mass (M) was measured using an electronic balance (ER-120A, AND, Japan) with 0.001 g sensitivity. Three linear dimensions (Figure

1), namely, length (L), width (W), and thickness (T), were measured with a digital Vernier calliper (Series 500, Mitutoyo, Japan) sensitive to 0.01 mm. The sphericity (Φ) and geometric mean diameter (D_g) were determined using Eqs. 1 - 2 (Tscheuschner and Mohseninm, 1987):

$$Dg = (LWT)^{\frac{1}{3}} \quad \text{(Eq. 1)}$$

$$\phi = \frac{(LWT)^{\frac{1}{3}}}{L} \quad \text{(Eq. 2)}$$

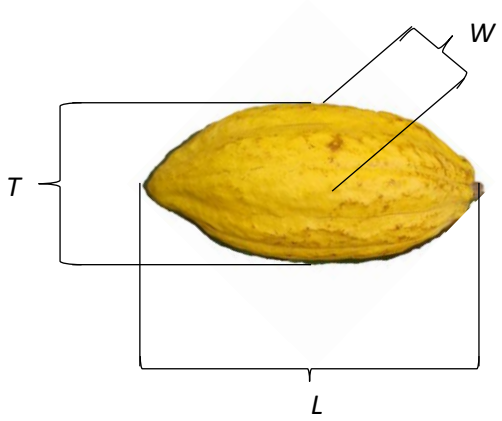

Figure 1. Principal dimensions of the cocoa fruit.

Two volume values were determined. Initially, the cocoa fruit was assumed to have a regular geometric shape, specifically an oblate spheroid (V_{obl}), or a prolate spheroid (V_{pro}). The volume was calculated using Eqs. 3 - 4 (Pathak *et al*., 2019).

$$V_{obl} = \frac{4\pi}{3}\left(\frac{L}{2}\right)\left(\frac{W}{2}\right)^2 \quad \text{(Eq. 3)}$$

$$V_{pro} = \frac{4\pi}{3}\left(\frac{L}{2}\right)\left(\frac{W}{2}\right)\left(\frac{T}{2}\right) \quad \text{(Eq. 4)}$$

The surface area of the cocoa fruit, which is equal to the total area of all surfaces with three-dimensional shapes, was determined using Eq. 5 (Azman *et al*., 2021).

$$SA_{sp} = \pi D_g^2 \quad \text{(Eq. 5)}$$

The projected areas perpendicular to thickness (PA_T), length (PA_L), and width (PA_W) were determined using Eqs. 6 - 8. The criterion-projected area (CPA) was then computed using Eq. 9. Azman *et al*. (2020) proposed the following equations:

$$PA_L = \frac{\pi LW}{4} \quad \text{(Eq. 6)}$$

$$PA_T = \frac{\pi TW}{4} \quad \text{(Eq. 7)}$$

$$PA_W = \frac{\pi WW}{4} \quad \text{(Eq. 8)}$$

$$CPA = \frac{PA_L + PA_T + PA_W}{3} \quad \text{(Eq. 9)}$$

Regression analysis and mass modelling

The four categories of models were used for mass modelling based on physical characteristics, projected area, volume, and surface area (Pathak *et al*., 2019):

i. Cocoa fruit mass was regressed in a single variable as a function of L, W, T, and geometric mean diameter (D_g).
ii. Based on projected cocoa fruit areas and CPA, a single-variable regression of cocoa fruit mass was performed.
iii. The fruit was assumed to be prolate spheroid (V_{pro}) or oblate (V_{obl}) in a single-variable regression analysis of cocoa fruit mass.
iv. The regression of cocoa fruit mass in a single variable was based on surface area.

The results of the experiments were used to fit four models: linear, quadratic, power, and S-curve models. The models are presented in Eqs. 10 - 13:

$$M = a + bX \quad \text{(Eq. 10)}$$

$$M = a + bX + cX^2 \quad \text{(Eq. 11)}$$

$$M = a + \frac{b}{X} \quad \text{(Eq. 12)}$$

$$M = aX^2 \quad \text{(Eq. 13)}$$

where, M = mass (g), X = independent variable (dimensions, volume, projected area, or surface area), and a, b, and c = curve-fitting parameters based on various equations.

Hot water blanching procedure

Short-time blanching using hot water was performed following previously described procedures (Delgado-Ospina *et al*., 2021). Briefly, CPH was processed by removing black spots from its pulp. CPH was then cut into 1 cm broad pieces, and then blanched using five various temperatures for several times (Table 1). The blanching process was

conducted using water bath (Memmert WNB 7-45). After blanching, the CPH was thawed and dried at 50°C until the moisture content reached 8 - 10%. The dried CPH was pulverised using a pulveriser machine (Retsch, SM200 Rostfrei, Germany), and passed through a stainless-steel sieve with a size of 80 mesh. The CPH powder was stored in cold storage at -5°C until further analyses.

Table 1. The most accurate and precise models for predicting the mass of cocoa based on a set of independent variables.

Dependent Parameter	Independent parameter	Model equation	Regression			Statistical parameters	
			a	b	c	R^2	SSE
M (g)	L (cm)	Quadratic	-0.34	0.06	-0.00	0.79	0.05
M (g)	T (cm)	Quadratic	1.30	-0.38	0.03	0.95	0.03
M (g)	W (cm)	Quadratic	0.92	-0.28	0.03	0.95	0.03
M (g)	Dg (cm)	Power	0.00	2.99	-	0.98	0.02
M (g)	V_{obl} (cm^3)	Quadratic	0.06	0.00	0.00	0.98	0.02
M (g)	V_{pro} (cm^3)	Quadratic	-0.01	0.00	-0.00	0.98	0.02
M (g)	SAsp (cm^2)	Quadratic	-0.11	0.00	0.00	0.98	0.02
M (g)	PA_L (cm^2)	Quadratic	-0.09	0.00	0.00	0.97	0.02
M (g)	PA_T (cm^2)	Quadratic	0.15	0.00	0.00	0.96	0.03
M (g)	PA_W (cm^2)	Quadratic	0.11	0.00	0.00	0.94	0.03
M (g)	CPA (cm^2)	Power	0.00	1.55	-	0.99	0.01

Experimental design and optimisation

The optimisation process for hot-water blanching was conducted using a Central Composite Design (CCD), a standard approach within Response Surface Methodology (RSM). This design was selected due to its efficiency in modelling quadratic relationships with minimal experimental runs, enabling an accurate evaluation of factor interactions (Ye *et al*., 2008). The design matrix generated 13 experimental runs. Each run was performed three times, and the average value was calculated. The number of tests was determined using Eq. 14 (Bhattacharya, 2021; Iwundu and Oko, 2021):

$$N = 2^k + 2k + C_0 \quad \text{(Eq. 14)}$$

where, k = number of independent variables, and C_0 = number of central points. Two independent variables—temperature (X_1) and time (X_2)—were considered. The responses: crude fibre, protein content, ash content, and moisture content were then evaluated.

The mathematical model used for analysing the influence of temperature and blanching time on responses (*e.g*., crude fibre and protein content) was a second-order polynomial equation expressed as:

$$Y = \beta_0 + \beta_1 X_1 + \beta_2 X_2 + \beta_{12} X_1 X_2 + \beta_{11} X_1^2 + \beta_{22} X_2^2 + \varepsilon \quad \text{(Eq. 15)}$$

where, Y = predicted response, β_0 = intercept, β_1 and β_2 = linear coefficients, β_{12} = interaction coefficient, β_{11} and β_{22} = quadratic coefficients, and ε = error term.

The predictive models for responses were validated using statistical parameters, including the coefficient of determination (R^2), bias factor, and average absolute deviation modulus (AADM). The bias factor was calculated using Eq. 16:

$$Bias = \frac{predicted\ value}{observed\ value} \quad \text{(Eq. 16)}$$

The AADM was calculated using Eq. 17:

$$AADM = \frac{\Sigma_{i=1}^{n} |observed\ value - predicted\ value|}{n} \quad \text{(Eq. 17)}$$

Chemical properties

pH level

The CPH pH levels were measured using the potentiometric method with a pH-determining suspension, and then titrated with 0.1 N NaOH solution until pH 8.2 was attained. The pH value was expressed as a percentage of oleic acid per 100 µL of sample (Salvador-Reyes and Paucar-Menacho, 2019).

Proximate composition

The proximate composition of CPH, such as moisture, protein, ash, crude fibre, and fat contents,

were determined following standard procedures of Association of Official Agricultural Chemists (AOAC, 1995). The moisture content of CPH was analysed using gravimetric methods, by allowing 5.0 g of the CPH sample to dry for 24 h at 105°C in an oven (Memmert, INB 200, Germany). The nitrogen content of cocoa pods was determined using a Kjeldahl apparatus (Kjeltec 2300, Foss Tecator, Denmark), and the amount of nitrogen was multiplied by 6.25 to determine the total protein in the CPH. Using the dry ashing method, the ash content of cocoa pods was assessed in a muffle furnace (Being, BWF 11/13 1100°C, USA) at 550°C for 90 min. The crude fat was calculated using a Soxhlet tool (Soxtec TM 2050, Denmark) with *n*-hexane as a solvent. The amount of carbohydrates was determined using the Anthrone method (Idris *et al*., 2021).

Antioxidant activity

The free-radical scavenging activity against DPPH was assessed by combining 5 mL of sample extract with 1 mL of freshly prepared 1 mM DPPH in methanol, and controls were prepared with 5 mL of 80% methanol and 1 mL of DPPH solution. After incubation in the dark for 30 min, absorbance was measured at 517 nm using a UV-visible spectrophotometer (Nie *et al*., 2021).

Total phenolic content

The TPC was measured using the Folin-Ciocalteu reagent method. Briefly, 0.2 mL of each 1 mg/mL sample extract was mixed with 10-fold diluted Folin-Ciocalteu reagent (1 mL) and 7.5% bicarbonate solution (0.8 mL). Absorbance at 765 nm was measured using a UV-visible spectrophotometer (Shimadzu UV1780, Japan), and the TPC was expressed in milligrams of gallic acid equivalents (GAE) per gram of dry matter (Yamin *et al*., 2021).

Dietary fibre

The dietary fibre content of CPH was determined using an enzymatic method based on AOAC methods 991.43 (K-TDFR, Megazyme). Initially, CPH samples were subjected to cold acetone extraction, air-dried, and powdered. Sequential enzymatic digestion was performed using heat-stable α-amylase, protease, and amyloglucosidase. Then, each sample was boiled with MES/TRIS buffer and α-amylase, and incubated with protease, and pH was adjusted with HCl. After further incubation with amyloglucosidase, the solution was filtered for the separation of insoluble (residue) and soluble (filtrate) fractions. Insoluble dietary fibre (IDF) was obtained by washing the residue with ethanol and acetone, dried, and weighed. The soluble dietary fibre (SDF) was quantified from the filtrate through HPLC coupled with a refractive index detector. Finally, the total dietary fibre was calculated as the sum of IDF and SDF. This method provides an accurate assessment of the dietary fibre content in CPH samples (Wattanavanitchakorn *et al*., 2023).

Statistical analysis

Data analysis and mass prediction were performed using a statistical software, such as SigmaPlot 12.0 (Systat Software Inc., Palo Alto, CA, USA), at a significance level of 1%. The accuracy of the regression model was assessed with the coefficient of determination (R^2) and standard error of estimate (SEE). The best model used was the model with a higher R^2 value, and a lower SEE value (Nur Salihah *et al*., 2015; Sujinda *et al*., 2021). The analysis of variance (ANOVA) was conducted with a confidence level of 95%, and the effect of each variable on the physicochemical properties of CPH was determined. ANOVA and parameter optimisation were performed with Minitab 16 (Minitab Inc., State College, PA, USA).

Result and discussion

Physical properties of cocoa

The mean L, W, and T values for cocoa were 14.86 ± 2.28, 7.77 ± 0.86, and 7.74 ± 0.84 cm, respectively. Among these, L exhibited the highest mean value, indicating that cocoa fruits had an elongated shape. These findings are critical for the design and optimisation of cocoa-handling equipment, particularly for roller-based sorting and grading systems, which require precise dimensional inputs to enhance efficiency (Mahawar *et al*., 2019).

The geometric mean diameter (Dg) averaged 9.78 ± 1.04 cm, while the sphericity was 0.65 ± 0.06. These values suggested that the shape of the cocoa fruit deviated significantly from a perfect sphere, aligning with similar observations in other tropical fruits like papaya and mango (Pathak *et al*., 2019). Such geometric characteristics are crucial for calculating volumetric properties and bulk storage requirements. The mass of the cocoa fruits averaged 0.41 ± 0.14 kg, with a wide range reflecting variability in fruit development.

The other physical characteristics of cocoa, including prolate and oblate spheroid volumes (493.11 ± 177.57 and 501.84 ± 170.7 cm^3, respectively), highlighted the need for approximating cocoa fruit as spheroidal shapes. This assumption supported efficient modelling for processing and storage applications, as previously reported for similar fruit geometries (Azman *et al*., 2020).

The average surface area (SAsp) was 296.53 ± 63.02 cm^2, while projected areas perpendicular to the three primary axes, such as PA_L, PA_T, and PA_W, were 91.01 ± 20.36, 48.48 ± 10.14, and 47.67 ± 10.46 cm^2, respectively. The criterion-projected area (CPA) was 64.23 ± 13.66 cm^2. These parameters are essential for the development of machine-vision grading systems, as they enable precise differentiation and categorisation of fruits based on size and shape attributes (Mahawar *et al*., 2019). Variability in these measurements may arise from natural differences in fruit growth and development.

Mass modelling

Table 1 presents cocoa mass modelling using dimensions, volumes, weight, surface areas, and projected areas. High R^2 values and low SEE values are associated with the best possible model fit, and a high R^2 value indicates the best-fitting model (near 1.00).

Modelling based on fruit dimensions

The quadratic model had the highest R^2 value, and lowest SEE value for thickness, with values of 0.95 and 0.03, respectively (Table 1). Panda *et al*. (2020) suggested a formula for calculating kendu fruit's mass based on its thickness. Similar models for date fruit and *Terminalia chebula* fruit were reported by Pathak *et al*. (2019); the models used thickness as a determining physical parameter to predict the geometric mean diameter of cocoa. These diameters fit the power model (Eq. 14) well, with R^2 and SEE values of 0.98 and 0.02, respectively.

$$M = 0.000453X^{2.99} \quad \text{(Eq. 14)}$$

The S-curve models had lower R^2 values than the fitted models in all dimensions. The lower R^2 values may be attributed to the absence of uniform cocoa mass proportional to its size (A'Bidin *et al*., 2020). Thus, cocoa must be measured by thickness and geometric mean diameter.

Modelling based on fruit volume

The prediction outcome of the cocoa pod mass based on its volumes (V_{obl} and V_{pro}) showed that the quadratic model was the best among the models in terms of R^2 value. Eq. 15 shows that the volume assumed to be shaped as an oblate spheroid volume (V_{obl}) had the highest R^2 value, and the lowest SEE (0.98 and 0.02, respectively), and Eq. 16 shows that the volume assumed to be shaped as a prolate spheroid volume (V_{pro}) had the highest R^2 value, and the lowest SEE (0.98 and 0.02, respectively). The resulting equations represent the best models of cocoa:

$$M = 0.06 + 0.0006X + 0.0000001X^2 \quad \text{(Eq. 15)}$$

$$M = -0.01 + 0.0009X - 0.00000002X^2 \quad \text{(Eq. 16)}$$

A quadratic form was comparable to the mass prediction of dried *Terminalia chebula* fruit (Pathak *et al*., 2019), kendu fruit (Panda *et al*., 2020), Sohiong (Vivek *et al*., 2018), and pepper berries (Azman *et al*., 2020; 2021).

Modelling based on fruit project areas

The power model containing CPA (Eq. 17) was the best model obtained, having a high R^2 value of 0.99, and SEE value of 0.01. To calculate the mass of cocoa, the quadratic model of PA_W, PA_L, and PA_T (Table 2) was selected as the best model.

$$M = 0.0007X^{1.55} \quad \text{(Eq. 17)}$$

Table 2. Physicochemical properties of cocoa pod husk.

Compound	Amount
pH	5.96 ± 0.01
Moisture content (%)	7.10 ± 0.55
Carbohydrate (%)	5.99 ± 0.01
Protein (%)	8.72 ± 0.01
Ash (%)	10.02 ± 0.09
Fat (%)	4.00 ± 0.44
Crude fibre (%)	47.45 ± 0.28
Dietary fibre (g/100g)	59.95 ± 0.21
Antioxidant activity (mg GAEAC/g)	122.99 ± 0.05
TPC (mg GAE/100 g)	517.60 ± 35.19

Physichochemical properties

The physichochemical characteristics of CPH were measured (Table 2), which included pH,

moisture content, carbohydrate, protein, ash, fat, crude fibre, dietary fibre, TPC, and antioxidant activity (DPPH). The pH of CPH was 5.96, indicating that it was slightly acidic. The proximate composition was 7.1% (moisture content), 5.99% (carbohydrate), 8.72% (protein), 10.02% (ash), 4% (fat), and 47.45% (crude fibre). CPH had quite high TPC (517.60 mg GAE/100 g). CPH exhibited an overall antioxidant activity of 122.99 ± 0.05 mg GAEAC/g (DPPH), and fairly high dietary fibre content (59.95 g/100 g). The pH values observed in the present work were generally similar to those reported by Delgado-Ospina *et al*. (2021), but the moisture, ash, dietary fibre, DPPH, and TPC contents were higher, whereas the carbohydrates, protein, and fat contents were lower.

Effect of blanching condition on protein content

The experimental results of the protein content for all 13 runs are shown in Table 3. The protein content for the different combinations of parameters ranged from 4.11 to 4.36%, and demonstrated relatively low variability (SD = 0.09) with a mean value of 4.20%. These results agreed with those of Delgado-Ospina *et al*. (2021), who reported that the protein content of CPH was approximately 4.85 - 6.48%. Protein content decreased significantly from 8.72 ± 0.01% (before blanching) to values ranging between 4.11 ± 0.13 and 4.36 ± 0.02% (after blanching) under different conditions, indicating a loss of approximately 50%. The blanching process resulted in a considerable decrease in CPH content possibly because of the leaching of soluble protein components into the discarded blanching water, and subsequent loss of some protein (Joshi and Joshi, 2016). The protein content of various products can add value from a nutritional standpoint.

Effect of blanching condition on crude fibre

The crude fibre content for the different combinations of parameters ranged from 34.68 to 35.93% (Table 3), showing slightly higher variability (SD = 0.40), with a mean of 35.29%, and reaching its highest value of 35.93%. These results agreed with those of Delgado-Ospina *et al*. (2021), who reported that the total fibre of CPH was approximately 35.3 - 37%. Pectin is primarily responsible for 30% of the total fibre in soluble fibre (Muñoz-Almagro *et al*., 2019). Akter *et al*. (2010) reported that the fibre content and swelling capacity of blanched dried persimmon peel were higher than those of unblanched dried persimmon peel. Blanched peel should be dehydrated to obtain high-quality dietary fibre powder from persimmon peel for use in food applications or in fibre-fortified food for health promotion.

Effect of blanching condition on moisture content

The moisture content for the different combinations of parameters ranged from 0.31 to 9.85% (Table 3), exhibiting the highest variability (SD = 2.81) among the responses, with values ranging widely from 0.31 to 9.85%. However, the temperature and time of blanching had no effect on the moisture content. This finding was consistent with that of a previous study (Gulzar *et al*., 2018), which showed that the moisture contents of mango and carrot slices were not considerably influenced by the blanching condition. According to Rosidi *et al*. (2021), blanched powdered samples had higher fibre, water activity, and moisture than an unblanched or blanched sample.

Effect of blanching condition on ash content

The ash content for the different combinations of parameters ranged from 5.08 to 7.24%, demonstrating a moderate standard deviation (SD = 0.57), and an average value of 5.89%. Ash content decreased from 10.02 ± 0.09% (before blanching) to values between 5.08 ± 0.08 and 7.24 ± 0.04%, with losses influenced by blanching conditions. The decrease likely resulted from mineral leaching due to prolonged exposure to water at high temperatures. However, the blanching time and temperature had no effect on the ash content ($p > 0.05$). This observation was in agreement with that of Del Rosario and Mateo (2019), who reported that hot-water blanching pre-treatments had no significant effects on the total amount of ash in seaweed powder. Müftügil (1985) reported that ash, ascorbic acid, chlorophyll, and dry matter were lost during blanching.

Analysis of variance

The analysis of variance indicated that both the equation and the real relationship between the response and important variables were accurate. The effect experiments were conducted in accordance with the design matrix, and the protein and crude fibre contents were well fitted in the second-order polynomial model. The values of F and *p* determine the significance of the coefficient term; the

Table 3. Experimental results of proximate composition.

Independent variable		Response variable				Predicted value			
Temperature (°C)	Time (s)	Protein (%)	Crude Fibre (%)	Moisture content (%)	Ash Content (%)	Protein (%)	Crude Fibre (%)	Moisture content (%)	Ash Content (%)
70	7.5	4.13 ± 0.11	35.60 ± 0.15	9.85 ± 0.12	5.80 ± 1.54	4.12	31.75	3.42	3.85
60	5	4.11 ± 0.13	34.81 ± 0.18	0.65 ± 0.03	6.74 ± 0.18	4.02	33.05	1.30	4.90
60	10	4.29 ± 0.07	34.79 ± 0.09	1.55 ± 0.14	5.78 ± 0.17	4.22	31.20	4.20	3.65
70	7.5	4.21 ± 0.03	35.28 ± 0.08	1.17 ± 0.57	5.63 ± 0.23	4.12	31.75	3.42	3.85
90	7.5	4.24 ± 0.12	35.63 ± 0.27	0.31 ± 0.01	5.58 ± 0.18	4.24	30.95	2.35	3.35
80	10	4.13 ± 0.11	35.67 ± 0.59	0.81 ± 0.09	5.64 ± 0.12	4.10	30.40	-0.60	2.25
70	12.5	4.36 ± 0.02	35.93 ± 0.72	0.81 ± 0.02	5.08 ± 0.08	4.22	30.20	-0.67	1.60
80	5	4.32 ± 0.06	35.34 ± 0.69	8.90 ± 0.07	7.24 ± 0.04	4.30	32.65	5.50	4.50
70	7.5	4.26 ± 0.09	35.36 ± 0.27	0.52 ± 0.06	5.33 ± 0.02	4.12	31.75	3.42	3.85
70	7.5	4.11 ± 0.10	35.19 ± 0.23	2.96 ± 0.11	6.14 ± 0.16	4.12	31.75	3.42	3.85
70	2.5	4.16 ± 0.06	35.50 ± 0.06	1.21 ± 0.02	5.33 ± 0.30	4.22	34.30	2.52	5.10
70	7.5	4.11 ± 0.09	35.17 ± 0.09	2.75 ± 0.15	5.94 ± 0.39	4.12	31.75	3.42	3.85
50	7.5	4.13 ± 0.10	34.68 ± 0.10	4.96 ± 0.20	6.66 ± 0.46	4.08	32.15	2.92	5.15

significance increases as F increases, and *p* decreases. The *p* value was less than 0.05, indicating that the model was statistically significant. The interaction between the temperature and blanching time significantly influenced protein content ($p > 0.05$), and the crude fibre was influenced by the linear effect of temperature ($p < 0.05$). The moisture and ash contents were not significantly influenced by temperature and time of blanching.

Model equation

The R^2 value is essential in the formulation and testing of equations and models for accurate response surface appropriateness. The R^2 values calculated for protein, crude fibre, moisture, and ash contents in the present work were 0.71, 0.82, 0.28, and 0.42, respectively. An R^2 value greater than 0.7 is acceptable for the development of an optimisation statistical model (Peng *et al*., 2020). According to the CCD and input variables, a quadratic equation for predicting the optimum point was obtained. Then, on the basis of the experimental findings, the following empirical relationship between the response and the independent variables in the coded units was presented:

i. Protein = 2.46 + 0.02 Temperature + 0.22 Time + 0.0001 Temperature*Temperature + 0.004 Time*Time - 0.004 Temperature*Time
ii. Crude Fibre = 33.50 + 0.07 Temperature - 0.43 Time - 0.0005 Temperature*Temperature + 0.02 Time*Time + 0.004 Temperature*Time
iii. Ash Content = 8.15 - 0.11 Temperature + 0.65 Time + 0.001 Temperature*Temperature - 0.02 Time*Time - 0.01 Temperature*Time
iv. Moisture = -55.8 + 0.94 Temperature + 7.48 Time - 0.002 Temperature*Temperature - 0.1 Time*Time - 0.09 Temperature*Time

The aforementioned prediction models illustrated the relationship between extraction temperature (X_1) and time (X_2) using measured parameters. The temperature of blanching had a positive effect on protein, crude fibre, ash, and moisture contents. Time of blanching had a positive effect on protein, ash, and moisture contents, and a negative effect on crude fibre content. The quadratic effect of temperature had a positive effect on protein and ash contents, and a negative effect on crude fibre and moisture contents. The quadratic effect of time had a positive effect on protein and crude fibre contents, and a negative effect on ash and moisture contents. The interactive effect of temperature and time had a positive effect only on crude fibre content, but it had a negative effect on protein, ash, and moisture contents.

The response surface plots in Figure 2 reveal the interactive effects of temperature and blanching time on the physico-chemical properties of CPH. Protein content (Figure 2a) increased with increasing temperatures, likely due to thermal denaturation exposing reactive sites that enhanced protein solubility. However, extended blanching times led to a decrease in protein content, likely attributed to leaching of soluble proteins into the blanching medium, consistent with previous findings by Szymanek *et al*. (2020). Crude fibre content (Figure 2b) increased with both higher temperatures and longer blanching times, possibly due to the thermal breakdown of the husk matrix which released insoluble fibres (Xie *et al*., 2023). Moisture content (Figure 2c) increased at higher temperatures, suggesting water absorption during short blanching intervals, but decreased with longer blanching times. Similarly, ash content (Figure 2d) initially increased with temperature, reflecting the release of mineral salts, but decreased with prolonged blanching due to mineral leaching, in accordance with the findings of Bikila *et al*. (2020).

The overlaid contour plot displays the interaction between blanching temperature and time for crude fibre and protein contents. The plot illustrates regions where both response variables meet the desired thresholds. The acceptable range for crude fibre (35.5 - 36.5%) and protein (4.1 - 4.4%) defines the shaded or overlapping area on the plot. This compromise region indicates the optimal combination of blanching conditions that simultaneously maximise crude fibre and protein retention. The contour lines for protein content show that higher temperatures (above 75°C) lead to increased protein denaturation, resulting in a narrower acceptable range for protein. Conversely, crude fibre content increases with longer blanching times, reflecting thermal breakdown of the husk matrix. The optimal region lies within blanching temperatures of approximately 78 - 80°C and times of 11 - 13 sec, where both responses meet the specified criteria.

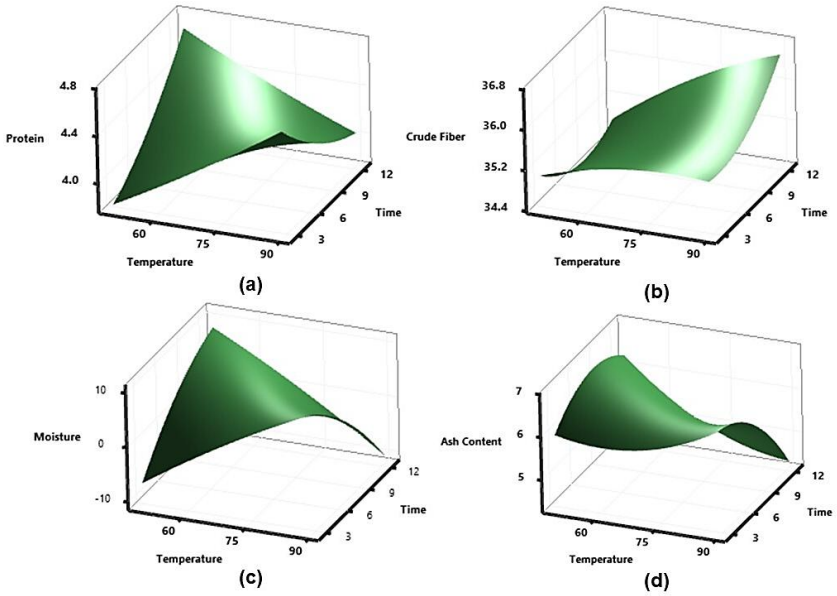

Figure 2. Response plots of process variables on protein **(a)**, crude fibre **(b)**, moisture **(c)**, and ash **(d)** contents.

Optimum condition

Only two parameter models among the four measured parameters were suitable for predicting the response value, namely protein and crude fibre. The high coefficient of determination confirmed the model's adequacy to predict protein and crude fibre contents. The identified optimal conditions—79°C for 12.5 sec—produced predicted values of 36.19% crude fibre and 4.19% protein. Experimental validation under these conditions yielded closely matched results of 50.13% crude fibre and 4.14% protein, demonstrating the model's reliability. The experimental and predicted values for protein and crude fibre content demonstrated the model's performance. The experimentally optimised protein content was 4.14%, closely matching the predicted value of 4.09%, with a deviation of 0.05%. Conversely, crude fibre content exhibited a larger discrepancy, with an experimental value of 36.19%, compared to the predicted value of 29.71%, resulting in a deviation of 6.48%. The Bias Factor for protein was 1.01, and the AADM was 0.05%, indicating excellent agreement between the predicted and observed values. In contrast, crude fibre content showed a Bias Factor of 0.72 and an AADM of 13.94%, indicating that the model underestimated the observed value by 28%. This discrepancy suggested the need for model refinement to better account for factors influencing fibre release during blanching.

The increase in crude fibre content at higher temperatures was likely due to the thermal degradation of the husk matrix, enhancing the availability of insoluble fibres (Muñoz-Almagro *et al*., 2019). Conversely, protein content may decrease slightly due to leaching of soluble protein fractions into the blanching medium, a common phenomenon during thermal processing (Eltom *et al*., 2023). Overall, CPH compounds subjected to hot-water blanching thermal treatment contained low amounts of compounds than CPH without treatment due to leaching or the loss of soluble compounds into the hot-water blanching media (Magangana *et al*., 2021). Therefore, the optimisation of thermal treatments, especially hot-water blanching, would minimise the loss of compounds from CPH during leaching, and retain the functional compounds in CPH.

Conclusion

The present work provided valuable insights into optimising hot-water blanching for cocoa pod husk (CPH), highlighting its potential as a source of crude fibber and bioactive compounds for health-related and industrial applications. At optimal blanching conditions (79°C for 12.5 sec), crude fibber content was maximised, and protein loss was minimised, demonstrating the efficacy of the response surface methodology (RSM) in balancing nutritional retention with processing efficiency. The developed models, including the non-linear equation for cocoa fruit mass and the prolate spheroid volume prediction model, would offer practical tools for improving post-harvest handling and equipment design. However, limitations such as the utilisation of

CPH samples from a single source, the absence of another antioxidant analysis (FRAP, ORAC, ROH), colour measurement, flavonoid content, polyphenol oxidase activity, and mineral content analyses, and a lack of comparisons with alternative blanching techniques, suggested opportunities for future research. Several blanching methods should be explored in the near future to provide a better understanding of the optimal method, improve nutrient retention, and expand the utilisation of CPH as a functional food ingredient, as a value-added by-product application.

Acknowledgement

The authors would like to specially thank Universiti Putra Malaysia for providing the research facilities and financial supports through the Grant Putra GP-IPS (grant no.: GP-IPS/2023/9748700), and UPM-SEARCA Scholarship (grant no.: GBG22-0923).

References

A'Bidin, F. N. Z., Shamsudin, R., Basri, M. S. M. and Dom, Z. M. 2020. Mass modelling and effects of fruit position on firmness and adhesiveness of banana variety Nipah. International Journal of Food Engineering 16(10): 20190199.

Akter, M. S., Ahmed, M. and Eun, J. B. 2010. Effect of blanching and drying temperatures on the physicochemical characteristics, dietary fiber composition and antioxidant-related parameters of dried persimmons peel powder. International Journal of Food Sciences and Nutrition 61(7): 702-712.

Andrade Sodré, G., Roberto, A. and Gomes, S. 2019. Cocoa propagation, technologies for production of seedlings. Revista Brasileira de Fruticultura 41(2): e-782.

Association of Official Analytical Chemists (AOAC). 1995. Official methods of analysis of the AOAC International. 14th ed. United States: AOAC.

Azman, P. N. M. A., Shamsudin, R., Che Man, H. and Ya'acob, M. E. 2021. Mass modelling of pepper berries (*Piper nigrum* L.) with some physical properties. Food Research 5: 80-84.

Azman, P. N. M. A., Shamsudin, R., Man, H. C. and Ya'acob, M. E. 2020. Some physical properties and mass modelling of pepper berries (*Piper nigrum* L.), variety Kuching, at different maturity levels. Processes 8(10): 1-15.

Belwal, T., Cravotto, C., Ramola, S., Thakur, M., Chemat, F. and Cravotto, G. 2022. Bioactive compounds from cocoa husk: Extraction, analysis and applications in food production chain. Foods 11(6): 1-13.

Bhardwaj, K., Najda, A., Sharma, R., Nurzyńska-Wierdak, R., Dhanjal, D. S., Sharma, R., … and Bhardwaj, P. 2022. Fruit and vegetable peel-enriched functional foods: Potential avenues and health perspectives. Evidence-Based Complementary and Alternative Medicine 2022: 543881.

Bhattacharya, S. 2021. Central composite design for response surface methodology and its application in pharmacy. In Kayaroganam, P. (ed). Response Surface Methodology in Engineering Science, p. 1-19. United Kingdom: IntechOpen.

Bikila, A. M., Tola, Y., Esho, T. B. and Forsido, S. F. 2020. Effect of predrying treatment and drying temperature on proximate composition, mineral contents, and thermophysical properties of anchote (*Coccinia abyssinica* (Lam.) Cogn.) flour. Food Science and Nutrition 8(10): 5532-5544.

Dahunsi, S. O., Osueke, C. O., Olayanju, T. M. A. and Lawal, A. I. 2019. Co-digestion of *Theobroma cacao* (cocoa) pod husk and poultry manure for energy generation: Effects of pretreatment methods. Bioresource Technology 283: 229-241.

Del Rosario, E. Z. and Mateo, W. 2019. Hot water blanching pre-treatments: Enhancing drying of seaweeds (*Kappaphycus alvarezii* S.). Open Science Journal 4(1): 1-25.

Delgado-Ospina, J., Lucas-González, R., Viuda-Martos, M., Fernández-López, J., Pérez-Álvarez, J. Á., Martuscelli, M. and Chaves-López, C. 2021. Bioactive compounds and techno-functional properties of high-fiber co-products of the cacao agro-industrial chain. Heliyon 7(4): e06799.

Eltom, H. A. E., Sulieman, M. A. and Hassan, A. B. 2023. Effect of boiling and roasting processing on nutritional quality of two Sudanese peanuts (*Arachis hypogaea*) cultivars. Legume Science 5(1): e159.

Gulzar, A., Ahmed, M., Qadir, M. A., Shafiq, M. I., Ali, S., Ahmad, I. and Mukhtar, M. F. 2018.

Effect of blanching techniques and treatments on nutritional quality of dried mango slices during storage. Polish Journal of Food and Nutrition Sciences 68(1): 5-13.

Hamzah, A. F. A., Hamzah, M. H., Man, H. C., Jamali, N. S. and Siajam, S. I. 2024. Influence of subcritical water pretreatment temperature on pineapple waste biogas efficiency: Experimental and kinetic study. Journal of Engineering and Sustainable Development 28(2): 143-159.

Idris, S. B., Shamsudin, R., Mohd Nor, M. Z., Mokhtar, M. N. and Abd Ghani, S. S. 2021. Proximate composition of different parts of white cassava (*Manihot esculenta* Crantz) plant as a ruminant feed. Advances in Agricultural and Food Research Journal 2(1): 1-9.

Iwundu, M. P. and Oko, E. T. 2021. Design efficiency and optimal values of replicated central composite designs with full factorial portions. African Journal of Mathematics and Statistics Studies 4(3): 89-117.

Joshi, K. and Joshi, I. 2016. Effect of blanching on nutritional composition of *rasbhari* (*Physalis peruviana*) fruit. Journal of Science and Technology 5(1): 29-33.

Khoshnam, F., Tabatabaeefar, A., Varnamkhasti, M. G. and Borghei, A. 2007. Mass modeling of pomegranate (*Punica granatum* L.) fruit with some physical characteristics. Scientia Horticulturae 114(1): 21-26.

Kim, A. N., Lee, K. Y., Rahman, M. S., Kim, H. J., Chun, J., Heo, H. J., … and Choi, S. G. 2020. Effect of water blanching on phenolic compounds, antioxidant activities, enzyme inactivation, microbial reduction, and surface structure of samnamul (*Aruncus dioicus* var. *kamtschaticus*). International Journal of Food Science and Technology 55(4): 1754-1762.

Magangana, T. P., Makunga, N. P., la Grange, C., Stander, M. A., Fawole, O. A. and Opara, U. L. 2021. Blanching pre-treatment promotes high yields, bioactive compounds, antioxidants, enzyme inactivation and antibacterial activity of 'wonderful' pomegranate peel extracts at three different harvest maturities. Antioxidants 10(7): 1119.

Mahawar, M. K., Bibwe, B., Jalgaonkar, K. and Ghodki, B. M. 2019. Mass modeling of kinnow mandarin based on some physical attributes. Journal of Food Process Engineering 42(5): e13079.

Müftügil, N. 1985. Effect of blanching and refrigerated storage temperature on the quality of frozen broad beans. International Journal of Refrigeration 8(4): 236-239.

Muñoz-Almagro, N., Valadez-Carmona, L., Mendiola, J. A., Ibáñez, E. and Villamiel, M. 2019. Structural characterisation of pectin obtained from cacao pod husk. Comparison of conventional and subcritical water extraction. Carbohydrate Polymers 217: 69-78.

Nhi, T. T. Y., Quy, N. N., Truong, L. D., Phat, D. T. and Phong, H. X. 2022. Comparison of pretreatment methods on total ascorbic acid, total phenolic content, and color of soursop (*Annona muricata* L.) pulp. Steam blanching, hot water blanching, and microwave-assisted blanching. Journal of Food Processing and Preservation 46(11): e17017.

Nie, J., Chen, D., Lu, Y. and Dai, Z. 2021. Effects of various blanching methods on fucoxanthin degradation kinetics, antioxidant activity, pigment composition, and sensory quality of *Sargassum fusiforme*. LWT - Food Science and Technology 143: 111179.

Nur Salihah, B., Rosnah, S. and Norashikin, A. A. 2015. Mass modeling of Malaysian varieties pomelo fruit (*Citrus grandis* L. Osbeck) with some physical characteristics. International Food Research Journal 22(2): 488-493.

Panda, G., Vivek, K. and Mishra, S. 2020. Physical characterization and mass modeling of *Kendu* (*Diospyros melanoxylon* Roxb.) fruit. International Journal of Fruit Science 20(S3): S2005-S2017.

Pathak, S. S., Pradhan, R. C. and Mishra, S. 2019. Physical characterization and mass modeling of dried *Terminalia chebula* fruit. Journal of Food Process Engineering 42(3): 1-10.

Peng, W. L., Mohd-Nasir, H., Setapar, S. H. M., Ahmad, A. and Lokhat, D. 2020. Optimization of process variables using response surface methodology for tocopherol extraction from Roselle seed oil by supercritical carbon dioxide. Industrial Crops and Products 143: 111886.

Rosidi, N. A. S., Abdul Ghani @ Yaacob, A., Yusof, N. and Yusof, N. (2021). Effect of blanching and drying temperatures on physicochemical properties of red dragon fruit (*Hylocereus*

polyrhizus) peel powder. Journal of Agrobiotechnology 12(1S): 62-73.

Rossetti, A. G., Moura, C. F. H., Silva, E. O., Vidal Neto, F. D. C., Ribeiro, L. B. and de Almeida, A. C. P. 2022. Sample size for the physical and physico-chemical characteristics of the cashew. Revista Brasileira de Fruticultura 44(6): e-614.

Salvador-Reyes, R. and Paucar-Menacho, L. M. 2019. Optimization of the blanching time and temperature in the manufacture of Hass avocado pulp using low quality discarded fruits. Brazilian Journal of Food Technology 22: 1-17.

Sujinda, N., Varith, J., Shamsudin, R., Jaturonglumlert, S. and Chamnan, S. 2021. Development of a closed-loop control system for microwave freeze-drying of carrot slices using a dynamic microwave logic control. Journal of Food Engineering 302: 110559.

Syamsiro, M., Saptoadi, H., Tambunan, B. H. and Pambudi, N. A. 2012. A preliminary study on use of cocoa pod husk as a renewable source of energy in Indonesia. Energy for Sustainable Development 16(1): 74-77.

Szymanek, M., Dziwulska-Hunek, A. and Tanaś, W. 2020. Influence of blanching time on moisture, sugars, protein, and processing recovery of sweet corn kernels. Processes 8(3): 340.

Tscheuschner, H.-D. and Mohseninm N. N. 1987. Physical properties of plant and animal materials. Structure, physical characteristics and mechanical properties. Food 31(7): 702-702.

Vivek, K., Mishra, S. and Pradhan, R. C. 2018. Physicochemical characterization and mass modelling of Sohiong (*Prunus nepalensis* L.) fruit. Journal of Food Measurement and Characterization 12(2): 923-936.

Wattanavanitchakorn, S., Wansuksri, R., Chaichoompu, E., Kamolsukyeunyong, W. and Vanavichit, A. 2023. Dietary fibre impacts the texture of cooked whole grain rice. Foods 12(4): 899.

Wibisono, Y., Diniardi, E. M., Alvianto, D., Argo, B. D., Hermanto, M. B., Dewi, S. R., … and Saiful, S. 2021. Cacao pod husk extract phenolic nanopowder-impregnated cellulose acetate matrix for biofouling control in membranes. Membranes 11(10): 748.

Xie, Y.-K., Li, X.-Y., Chen, C., Zhang, W.-P., Yu, X.-L., Xiao, H.-W. and Lu, F.-Y. 2023. Effects of steam and water blanching on drying characteristics, water distribution, microstructure, and bioactive components of *Gastrodia elata*. Plants 12(6): 1372.

Xu, Y. 2017. Textural and microbiological qualities of vegetable soybean (edamame) affected by blanching and storage conditions. Journal of Food Processing and Technology 3: 7.

Yamin, R., Mistriyani, S., Ihsan, S., Armadany, F. I., Sahumena, M. H. and Fatimah, W. O. N. 2021. Determination of total phenolic and flavonoid contents of jackfruit peel and *in vitro* antiradical test. Food Research 5(1): 84-90.

Ye, Z., Lu, M., Zheng, Y., Li, Y. and Cai, W. 2008. Lactic acid production from dining-hall food waste by *Lactobacillus plantarum* using response surface methodology. Journal of Chemical Technology and Biotechnology 83(11): 1541-1550.